Available online at www.sciencedirect.com
SCIENCE DIRECT®
Journal of Controlled Release 91 (2003) 439–448
journal of controlled release
www.elsevier.com/locate/jconrel

Ion-exchange fibers and drugs: a transient study

M. Vuorio[a,*], J.A. Manzanares[b], L. Murtomäki[a], J. Hirvonen[c], T. Kankkunen[c], K. Kontturi[a]

[a]*Laboratory of Physical Chemistry and Electrochemistry, Helsinki University of Technology, P.O. Box 6100, FIN-02015 HUT, Finland*
[b]*Department of Thermodynamics, University of Valencia, E-46100 Burjasot, Spain*
[c]*Department of Pharmacy, Pharmaceutical Technology Division and Viikki Drug Discovery Technology Center, University of Helsinki, P.O. Box 56, FIN-00014 Helsinki, Finland*

Received 14 March 2003; accepted 27 May 2003

Abstract

The objective of this study was to theoretically model and experimentally measure the kinetics and extent of drug release from different ion-exchange materials using an in-house-designed flow-cell. Ion-exchange fibers (staple fibers and fiber cloth) were compared with commercially available ion-exchange materials (resins and gels). The functional ion-exchange groups in all the materials were weak –COOH or strong $-SO_3H$ groups. The rate and extent of drug release from the fibers (staple fiber>fiber cloth) was much higher than that from the resin or the gel. An increase in the hydrophilicity of the model drugs resulted in markedly higher rates of drug release from the fibers (nadolol>metoprolol>propranolol>tacrine). Theoretical modelling of the kinetics of ion exchange provided satisfactory explanations for the experimental observations: firstly, a change in the equilibrium constant of the ion-exchange reaction depending on the drug and the ion-exchange material and, secondly, a decrease in the Peclet number (*Pe*) with decreasing flow-rate of the drug-releasing salt solution.

Keywords: Controlled release; Drug delivery; Ion-exchange fiber; Kinetics; Modelling

1. Introduction

Ion-exchange fibers were developed as suppressor materials for ion-exchange chromatography, improving the baseline stability and decreasing ion-exclusion effects and chemical reactions [1]. Fibers have been widely used in many applications due to their high separation capacity, fast ion-exchange rate and good electrical conductivity [2]. The applications of such fibers are wide ranging and include the separation of rare earth elements [3], enrichment of uranium from seawater [2], purification of air by the removal of acidic or alkaline impurities [4] and chromatographic methods [5–7]. Recently, it has also been proposed to use ion-exchange fibers in medical and pharmaceutical applications, e.g. as a drug reservoir in an iontophoretic patch for transdermal drug delivery [8–10].

The ion-exchange mechanism is assumed to be analogous to a liquid–solid phase reaction. In the case where Na^+ is in the solution and drug (D^+) is in the fiber, in the first stage the Na^+ ions diffuse to the solid surface through the solution (1). The Na^+

*Corresponding author.
E-mail address: marja.vuorio@hut.fi (M. Vuorio).

0168-3659/03/$ – see front matter
doi:10.1016/S0168-3659(03)00270-0

ions then diffuse inside the solid phase (2), which is followed by a chemical exchange reaction between the Na^+ and D^+ ions in the ion-exchange groups (3). Finally, the exchanged D^+ ions diffuse back into the solution. If (1) is the rate-determining step (RDS), the kinetics of the ion-exchange reaction are said to be ''liquid-film diffusion controlled'', if (2) is the RDS, the reaction is said to be ''particle diffusion controlled'' and in the case of (3) being the RDS, it is ''chemical reaction controlled''.

Even though ion-exchange kinetics is a widely researched topic [11–17], there have been few reports on the kinetics of ion-exchange fibers [2,18], possibly because the fibrous ion exchangers are relatively new materials. Information in English is especially scarce as much of the research on ion-exchange fibers has been published in China [19], Japan [20,21] and in Eastern European countries [22,23]. Most ion-exchange processes in resins are controlled by particle diffusion [18], which also appears to be the case for fibers. Chen et al. [2] suggested that the enhanced rate of ion exchange in the fibers is due to the smaller shell thickness of the fiber as compared to the resin, thus allowing the ions rapid access to the ion-exchange groups. Also, fibrous ion-exchange materials are suggested to have a larger surface area to unit volume ratio, which leads to a higher absorption rate and absorption capacity as compared to the resin [18].

For particle diffusion control, Helfferich [24] suggested ''a moving boundary'' or ''shell-progressive'' mechanism. This model is analogous to the mechanism presented by Weisz et al. [25] for the combustion of carbonaceous deposits within porous particles. The model presumes that counter-ions in the solution diffuse into the spherical ion-exchange bead, reacting with the ion-exchange groups forming a sharp boundary between the reacted and unreacted core, which advances from the surface of the particle to the center. The rate equation based on Helfferich's theory was later proved to fit the experimental data [15,26–28]. The theory was valid for spherical bead particles.

The earlier kinetic studies of ion-exchange fibers employed a finite solution volume method in stirred vessels [8,9,18]. In the present work, a flow-through cell was constructed after the example of chromatographic methods and flow experiments given by Krongautz et al. [14]. The objective of this study was to theoretically model and experimentally measure the kinetics (rate and extent) of drug release from different ion-exchange materials which were staple fibers, a fiber cloth, an ion-exchange resin and a gel. The present case is particular and has not previously been described mathematically. The cationic model drugs of varying lipophilicity were tacrine, propranolol, metoprolol and nadolol.

2. Experimental methods

2.1. Materials

The ion-exchange fiber materials employed were Smopex®-102, a poly(ethylene-*g*-acrylic acid) fiber, and -101, a poly(ethylene-*g*-styrenesulfonic acid) fiber (both from Smoptech, Turku, Finland), either in the form of staple or cloth. The other ion-exchange materials used were Amberlite IRC-86 gel and Diaion WK100 highly porous resin (both from Supelco, Bellefonte, PA, USA). All the materials contained carboxylate ion-exchange groups, except Smopex®-101, which contained sulfonic acid groups. The cationic model drugs were tacrine (–HCl), propranolol (–HCl), metoprolol (–tartrate) and nadolol (all from Sigma, St. Louis, MO, USA). The physicochemical properties of the drugs (molecular weight, dissociation constant, octanol/water partition coefficient) are presented in Table 1. The salt solution was NaCl (P.A. grade, Merck, Germany). Deionized Milli-Q® water (Millipore, Molsheim,

Table 1
Physicochemical properties of the studied drugs [33]

Drug	Molecular weight (g/mol)	Dissociation constant (pK_a)	Octanol/water partition coefficient (log P)
Tacrine	198.27	9.8±0.2 [8]	3.30[a]
Propranolol	259.35	9.45	3.56[a], 2.75[b]
Metoprolol	267.37	9.70	1.88[a], 1.20[b]
Nadolol	309.41	9.39	0.71[a], 0.23[b]

[a] Determined experimentally.
[b] Calculated using CLOGP version 3.54.

France) with a resistivity of ≥18 MΩ/cm was used to prepare all the solutions.

2.2. Determination of drug release kinetics in the flow-cell

Loading of the model drugs into the ion-exchange materials was performed by the same method as described previously [8], by immersing them in a 1 wt-% drug solution for 24 h. The amount of drug-containing ion-exchange material to be used in the kinetic experiments was calculated and weighed so that each sample contained the same molar amount of drug (1 mM). The ion-exchange material under analysis was placed inside the specially constructed flow-cell (Fig. 1). The NaCl solution (0.15 M) was pumped (Peristaltic pump Model IPN-12, Ismatec SA Laboratoriumstechnik, Switzerland) through the cell at varying flow-rates (0.1–5.0 ml/min). The resulting mixture of salt and drug was typically gathered for 3–172 h (depending on the flow-rate) using a Gilson FC203R fraction collector (Gilson, USA). Drug concentrations were analysed by HPLC (Waters, Milford, MA, USA) using chromatographic conditions similar to those reported earlier [8,9]. The drugs were analysed with a Waters Nova-Pak C_{18} column (150×3.9 mm, 4 μm). The analytical wavelength for tacrine, propranolol, metoprolol and nadolol was 254 nm. The flow-rate was 1.0 ml/min in each case.

The theoretical basis for the modeling of drug release from the ion-exchange materials (equilibrium constant and kinetics of ion exchange) is presented in detail below.

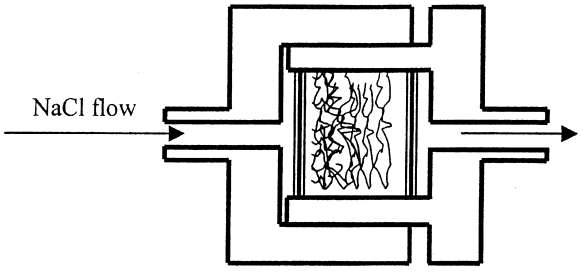

Fig. 1. In-house-designed flow-cell used for the drug release measurements. Porous sinters (triple line) were used on both sides of the ion-exchange matrix (curly line in the middle of the cell) to distribute the NaCl solution flow evenly inside the cell.

3. Theory

3.1. Equilibrium of drug release

The release of a cationic drug, D^+, takes place via the ion-exchange mechanism

$$D^+(\text{fiber}) + Na^+(w) \equiv D^+(w) + Na^+(\text{fiber}) \quad (1)$$

At (Donnan) equilibrium the chemical potentials of D^+ and Na^+ in the fiber and water phases are equal:

$$\begin{cases} \bar{\mu}^0_D + RT \ln \bar{c}_D + F\bar{\phi} = \mu^0_D + RT \ln c_D + F\phi \\ \bar{\mu}^0_{Na} + RT \ln \bar{c}_{Na} + F\bar{\phi} = \mu^0_{Na} + RT \ln c_{Na} + F\phi \end{cases} \quad (2)$$

In Eq. (2), the overbar denotes the fiber phase. Subtracting these equations from each other, the Galvani (Donnan) potential drop ($\bar{\phi} - \phi$) can be eliminated; it cannot be measured:

$$(\bar{\mu}^0_D - \mu^0_D) - (\bar{\mu}^0_{Na} - \mu^0_{Na}) = \Delta\mu^0_D - \Delta\mu^0_{Na} = RT \ln \frac{c_D \bar{c}_{Na}}{\bar{c}_D c_{Na}} \quad (3)$$

Rearranging (3) gives

$$K = \exp\left[\frac{1}{RT}(\Delta\mu^0_D - \Delta\mu^0_{Na})\right] = \frac{P^0_{Na}}{P^0_D} = \frac{c_D \bar{c}_{Na}}{\bar{c}_D c_{Na}} \quad (4)$$

where P^0 is the partition coefficient between the water and fiber phases; thus K is the equilibrium constant of reaction (1). It seems that the value of K depends on the nature of the ion-exchange matrix. In the chemical potential, concentrations should be replaced by activities, but the activity coefficients can be included in the value of P^0.

3.1.1. Kinetics of ion exchange

The exchange reaction (1) is presumably very fast compared to the rate of diffusion [29]. Therefore, the Donnan equilibrium can be assumed to be valid on the surface of the fiber. The kinetic problem is, therefore, reduced to a transport problem, which is still far from trivial to solve. The molar flux density

J_i of ionic species i is described in terms of the Nernst–Planck equation:

$$-j_i = \nabla c_i + z_i c_i \frac{F}{RT} \nabla \phi - \frac{u c_i}{D_i} \quad (5)$$

where $j_i = J_i/D_i$, D_i is the diffusion coefficient of species i, u is the convective solution velocity.

As the fiber is in the form of an entangled bunch or coil, through which the solution flows, it is impossible to solve Eq. (5) exactly. Therefore, we treat the patch of fiber as a ''black box'' with an effective surface area $\bar{A}$ and of diffusion boundary layer thickness δ. Eq. (5) is used in a unidimensional form, replacing the gradient operator ∇ with the derivative $\mathrm{d}/\mathrm{d}x$, where x is the perpendicular distance from the fiber surface. Note that the classical term diffusion boundary layer is used here even though convection is present throughout the whole membrane system. The solution of these equations in the diffusion boundary layer must satisfy the electroneutrality condition:

$$c_2 = c_1 + c_3 \quad (6)$$

where the subscript 1 represents Na^+, $2Cl^-$ and 3 the ionic form of the drug, D^+. For the sake of simplicity, several approximations are used, reducing the number of fitting parameters, whilst taking into account the fact that the drug species diffuse more slowly than the other electrolyte ions. Firstly, the diffusion coefficients are given by the values $D_1 = D_2 = 2D_3 \equiv D$. Secondly, the Goldman constant electric field assumption is introduced, so that the Nernst–Planck equations are no longer coupled through the migration term. The electric field in $RT/F\delta$ units is denoted by E, $E \equiv -(F\delta/RT)(\nabla \phi)$, and must be evaluated from the open circuit condition, $I = F(J_1 - J_2 + J_3) = 0$. The Cl^- ion is considered to be completely excluded from the ion-exchange fiber, so that $P_2^0 = 0$ and $J_2 = 0$.

Taking $x = 0$ at the fiber–external solution interface, Eq. (5) is solved for $i = 2$ as

$$c_2^{\mathrm{b}} = c_2^{\mathrm{s}} e^{Pe-E} \quad (7)$$

where $Pe \equiv u\delta/D = \dot{V}\delta/D\bar{A}$ is the Peclet number and $\dot{V}$ denotes the volume flow; $c_2^{\mathrm{s}} = c_2(0)$ and $c_2^{\mathrm{b}} = c_2(\delta)$. Superscripts b and s denote the bulk aqueous phase and the interface, respectively. It is worth noting that the Peclet number conceals all the simplifying assumptions made above. Theoretically, it would take values of the order of 10^{-2}–10^{-3} if the true geometrical surface area reported by the manufacturer (ca. 3 m^2/g) were used, but as can be seen later, values of the order of 1–10 are found in the fits.

To solve the time-dependent problem, we should take the divergence of Eq. (5). The resulting group of partial differential equations would be very difficult to solve and, therefore, a quasi-stationary state assumption is adopted. This amounts to assuming that the flux density, J_i, is independent of position within each time interval Δt (see below). This assumption is rather good except at the very beginning of an experiment, when an initial burst of drug is released from the fiber. The time scale of the experiment is, however, much longer than the duration of the initial transient stage, and it can be neglected within the accuracy of the experiment.

Under this quasi-stationary state approximation and remembering that $D_1 = D_2 = 2D_3 \equiv D$, the transport equations for Na^+ and D^+ can be solved similarly and lead to the expressions

$$c_1^{\mathrm{b}} = \frac{j_1\delta}{Pe+E} + \left(c_1^{\mathrm{s}} - \frac{j_1\delta}{Pe+E}\right)e^{Pe+E} \quad (8a)$$

$$c_3^{\mathrm{b}} = \frac{j_3\delta}{2Pe+E} + \left(c_3^{\mathrm{s}} - \frac{j_3\delta}{2Pe+E}\right)e^{2Pe+E} \quad (8b)$$

These equations can be solved for the flux densities and lead to

$$j_1 = \frac{Pe+E}{\delta}\frac{c_1^{\mathrm{b}} - c_1^{\mathrm{s}}e^{Pe+E}}{1-e^{Pe+E}} \quad (9a)$$

$$j_3 = \frac{2Pe+E}{\delta}\frac{c_3^{\mathrm{b}} - c_3^{\mathrm{s}}e^{2Pe+E}}{1-e^{2Pe+E}} \quad (9b)$$

Since the electric current density is zero, $I = \Sigma_i z_i D_i j_i = 0$, the value of E can be obtained from the numerical solution of

$$2(Pe+E)\frac{c_1^{\mathrm{b}} - c_1^{\mathrm{s}}e^{Pe+E}}{1-e^{Pe+E}} + (2Pe+E)\frac{c_3^{\mathrm{b}} - c_3^{\mathrm{s}}e^{2Pe+E}}{1-e^{2Pe+E}} = 0 \quad (10)$$

At this stage it is more convenient to change to dimensionless variables $y_k = c_k/c^0$, where c^0 is the salt concentration in the feeding solution. Similarly,

the concentration of ionic species inside the membrane divided by the fixed charge concentration is represented by $\bar{y}_i = \bar{c}_i/\bar{c}_0$. Initially, $y_3^- = 1 - y_1^- = 1$, $y_3^b = 0$ and $y_1^b = y_2^b = 1$. When the fiber is immersed in the aqueous phase, if we assume that the kinetics is very fast, then the D^+ bound to the fiber is immediately replaced by Na^+. Therefore, initially $y_1^s = 0$, because the diffusion is too slow to compensate for the amount of Na^+ exchanged into the fiber. Since electroneutrality is also satisfied at the interface, Eq. (7) implies that, initially,

$$y_3^s = y_2^s = e^{E-Pe} \tag{11}$$

where E is obtained from the solution of Eq. (10) at $t = 0$, which reduces to

$$\frac{2(Pe+E)}{1-e^{Pe+E}} = \frac{(2Pe+E)e^{Pe+2E}}{1-e^{2Pe+E}} \tag{12}$$

After the initial stage, the Donnan equilibrium dictates the relationship between the surface concentrations. Eq. (4) can be written in the form

$$K = \frac{y_1^s \bar{y}_3}{y_3^s \bar{y}_1} = \frac{y_1^s \bar{y}_3}{y_3^s(1-\bar{y}_3)} \tag{13}$$

Using the electroneutrality condition $y_1^s = y_2^s - y_3^s$, this expression can also be written as

$$y_3^s = \frac{y_2^s \bar{y}_3}{(1-\bar{y}_3)K + \bar{y}_3} \tag{14}$$

To evaluate the time dependence of different concentrations, mass balances need to be considered. For the drug and Na^+ ions, $i = 1$ and 3, inside the membrane:

$$-\frac{\mathrm{d}\bar{n}_i}{\mathrm{d}t} = J_i \bar{A} \tag{15}$$

where $\bar{A}$ is the effective area of the fiber and $\bar{n}_i = \bar{V}\bar{c}_i$. Because we want to compare different convection rates, $\dot{V}$, we change the time scale to the amount of salt introduced into the cell:

$$\mathrm{d}n_{\mathrm{salt}} = \dot{V} c^0 \, \mathrm{d}t \tag{16}$$

Eq. (15) is then transformed into

$$-\frac{\mathrm{d}\bar{y}_1}{\mathrm{d}n_{\mathrm{salt}}} = \frac{j_1 \delta}{Pe\, \bar{n}_0} \tag{17a}$$

$$-\frac{\mathrm{d}\bar{y}_3}{\mathrm{d}n_{\mathrm{salt}}} = \frac{j_3 \delta}{2Pe\, \bar{n}_0} \tag{17b}$$

and, outside the membrane, we have

$$\frac{\mathrm{d}y_1^b}{\mathrm{d}n_{\mathrm{salt}}} = \frac{j_1 \delta}{Pe\, n_0} + \frac{1-y_1^b}{n_0} \tag{18a}$$

$$\frac{\mathrm{d}y_3^b}{\mathrm{d}n_{\mathrm{salt}}} = \frac{j_3 \delta}{2Pe\, n_0} - \frac{y_3^b}{n_0} \tag{18b}$$

The following iterative procedure is now employed:

Step 1 E is calculated from Eq. (12).

Step 2 Insert the initial values of all the quantities as old values to obtain the new ones by means of the following expressions (taking salt increments Δn_{salt}):

$$\bar{y}_{3,\mathrm{new}} = \bar{y}_{3,\mathrm{old}} - \frac{1}{2\bar{n}_0}\left[\left(2+\frac{E}{Pe}\right)\frac{y_3^b - y_3^s e^{2Pe+E}}{1-e^{2Pe+E}}\right]_{\mathrm{old}} \Delta n_{\mathrm{salt}}$$

$$y_{3,\mathrm{new}}^b = y_{3,\mathrm{old}}^b + \frac{1}{2n_0}\left[\left(2+\frac{E}{Pe}\right)\frac{y_3^b - y_3^s e^{2Pe+E}}{1-e^{2Pe+E}} - y_3^b\right]_{\mathrm{old}} \Delta n_{\mathrm{salt}}$$

$$y_{1,\mathrm{new}}^b = y_{1,\mathrm{old}}^b + \frac{1}{n_0}\left[\left(1+\frac{E}{Pe}\right)\frac{y_1^b - y_1^s e^{Pe+E}}{1-e^{Pe+E}} + 1 - y_1^b\right]_{\mathrm{old}} \Delta n_{\mathrm{salt}}$$

$$y_{2,\mathrm{new}}^b = y_{1,\mathrm{new}}^b + y_{3,\mathrm{new}}^b$$

$$y_{2,\mathrm{new}}^s = y_{2,\mathrm{new}}^b e^{E-Pe}$$

$$y_{3,\mathrm{new}}^s = \frac{y_{2,\mathrm{new}}^s \bar{y}_{3,\mathrm{new}}}{(1-\bar{y}_{3,\mathrm{new}})K + \bar{y}_{3,\mathrm{new}}}$$

$$y_{1,\mathrm{new}}^s = y_{2,\mathrm{new}}^s - y_{3,\mathrm{new}}^s$$

Step 3 Solve Eq. (10) numerically using the new values of the concentrations obtained in step 2 to obtain the new value of E.

Step 4 Go to step 2 for the next salt increment inserting all these calculated values as old values.

n_0 and $\bar{n}_0$ are always taken as 1.0.

4. Results and discussion

4.1. Tacrine

Fig. 2a–c show the experimental and modelled curves for tacrine release at different flow-rates and Table 2 shows the corresponding values of *Pe* and *K* for the four carboxylic acid-containing ion-exchange materials. A high value of *K* indicates that the equilibrium in Eq. (1) is on the right; the drug prefers the solution phase over the ion-exchange phase. Alternatively, a low value of *Pe* indicates a decrease in flow-rate. In all cases the Peclet number is the main fitting parameter, the partition coefficient *K* is not allowed to vary for a given pair of drug species and ion-exchange material. From Fig. 2a–c it is clear that the release rate of tacrine was higher from the small pieces of staple fiber than from the woven fiber cloth. Furthermore, the release of tacrine from the three-dimensional network forming gel and resin systems occurred at a significantly lower rate. As the flow of NaCl solution was increased from 0.1 to 1.0 ml/min, the rate and extent of tacrine release were increased accordingly. However, a further increase in the flow-rate to 5.0 ml/min did not improve the release of tacrine from the ion-exchange materials. A possible explanation for this is that ion-exchange kinetics start to affect the release rate of tacrine.

As noted in our earlier paper [9], tacrine has a strong interaction with the fibers and, apparently, also with the other ion-exchange materials. The release rates of tacrine were the slowest from all the matrices as compared to the release rates of the other drugs with the same flow rates of NaCl solution (see results below). Tacrine differs from the other model drugs studied, because it does not contain hydroxyl groups in the structure. The β-blocking agents have bulky, flexible and fairly polar substituents in the aromatic ring. The bulkiness of the substituent may be visualised, e.g. by comparing the estimated van der Waals volumes of the substances. The volumes

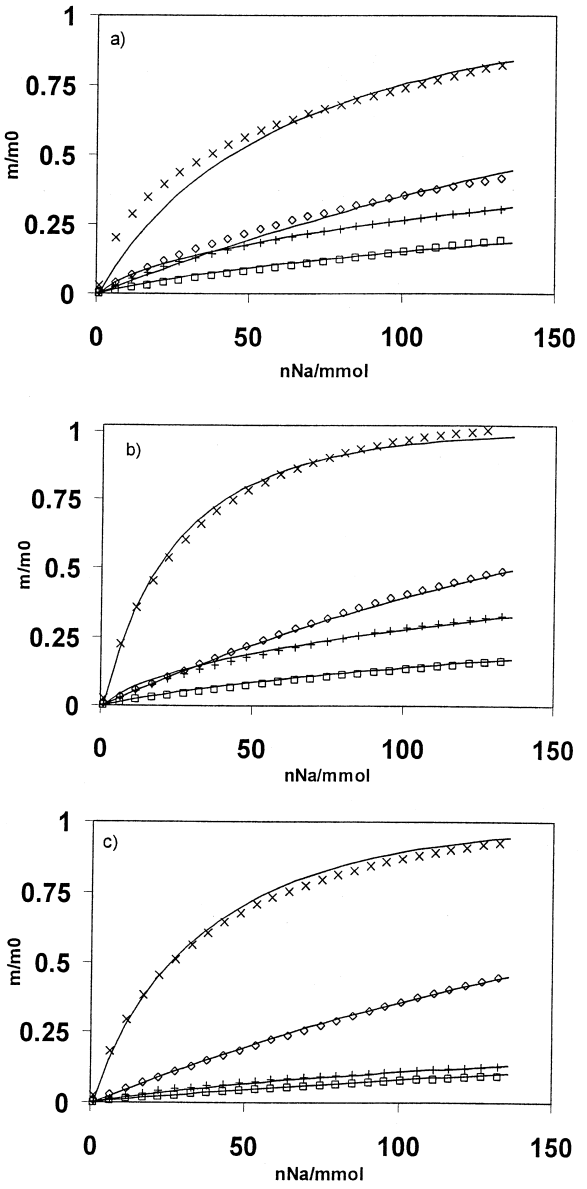

Fig. 2. Experimental [(×) staple 102, (◇) cloth 102, (+) gel and (□) resin] and theoretical (———) fractions of tacrine released as a function of the amount of Na^+ flow through the cell. Flow-rates: (a) 0.1 ml/min, (b) 1 ml/min, (c) 5 ml/min.

Table 2
Parameters *Pe* and *K* used for the modelling of tacrine release

	$\dot{V}$ (ml/min)	*Pe*	*K*
Smopex®-102, staple fiber	0.1	4.0	1.9
	1	3.1	1.9
	5	3.5	1.9
Smopex®-102, fiber cloth	0.1	5.5	1.0
	1	5.3	1.0
	5	5.5	1.0
Amberlite IRC-86 gel	0.1	4.8	16
	1	4.7	16
	5	6.3	16
Diaion WK100 resin	0.1	6.0	10
	1	6.1	10
	5	6.8	10

for nadolol, propranolol and tacrine were evaluated as 275, 245 and 160 $Å^3$, respectively [30].

4.2. Propranolol

Fig. 3a–c show the experimental and modelled curves for propranolol release with different flow rates and Table 3 shows the corresponding values of *Pe* and *K*. The Peclet number decreased with decreasing flow-rate, as the definition of the Peclet number suggests ($Pe = \dot{V}\delta/D\bar{A}$). The release of propranolol was significantly higher from the ion-exchange fiber than from the ion-exchange gel (Fig. 3a–c). However, the flow-rate of the NaCl solution did not present as profound effect on the release profiles as was observed with tacrine.

4.3. Metoprolol

Fig. 4 shows the experimental and modelled curves of metoprolol release using a NaCl solution flow-rate of 5 ml/min. Table 4 shows the corresponding values of *Pe* and *K*. The release rates of metoprolol from the carboxylate groups of the ion-exchange fiber were much higher than the corresponding release rates of tacrine or propranolol. The release rates of metoprolol from the ion-exchange gel and resin were, once again, significantly lower as compared to the fiber.

Metoprolol was also the model drug used to compare the rate of ion-exchange kinetics by strong (–SO_3H, Smopex®-101) and weak (–COOH, Smopex®-102) ion-exchange fibers. The release profiles of metoprolol from these fibers were fairly similar (Fig. 4). Previously, more pronounced differences were observed between strong and weak ion

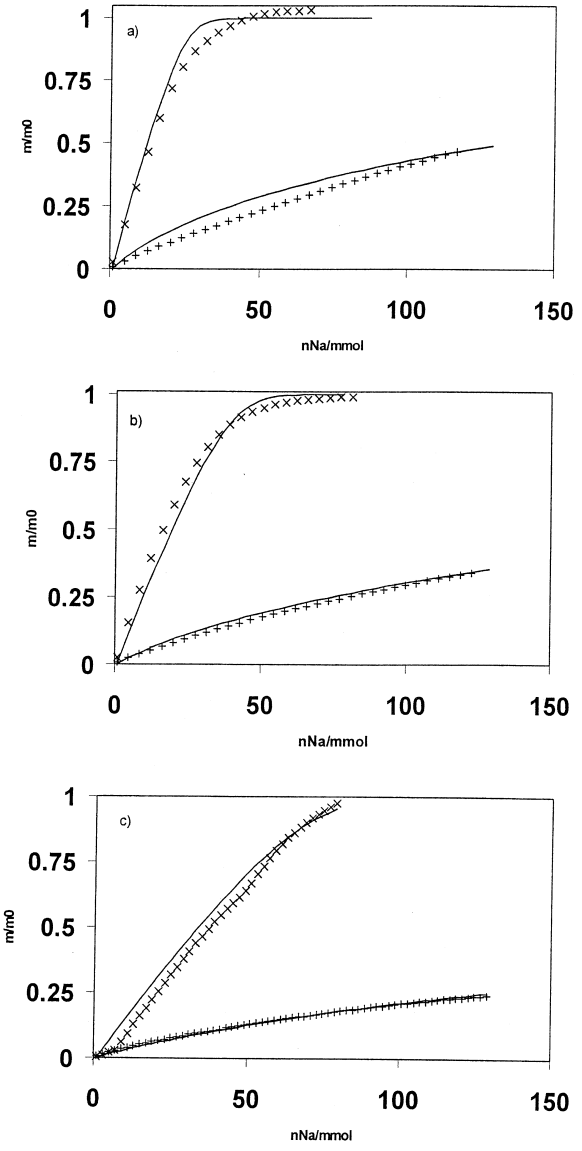

Fig. 3. Experimental [(×) staple 102 and (+) gel] and theoretical (———) fractions of propranolol released as a function of the amount of Na^+ flow through the cell. Flow-rates: (a) 0.1 ml/min, (b) 1 ml/min, (c) 5 ml/min.

Table 3
Parameters *Pe* and *K* used for the modelling of propranolol release

	$\dot{V}$ (ml/min)	*Pe*	*K*
Smopex®-102 fiber	0.1	3.4	0.15
	1	3.7	0.15
	5	4.2	0.15
Amberlite IRC-86 gel	0.1	4.6	4.8
	1	5.2	4.8
	5	5.8	4.8

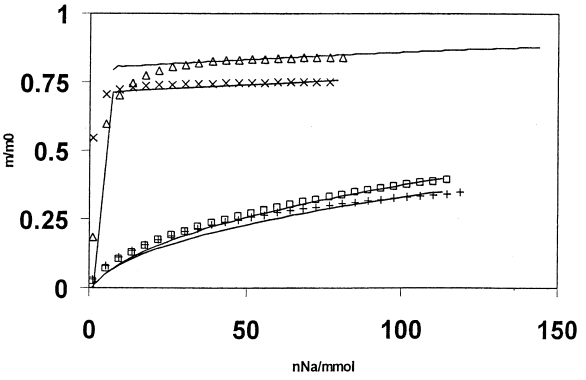

Fig. 4. Experimental [(×) staple 102, (△) staple 101, (+) gel and (□) resin] and theoretical (———) fractions of metoprolol released as a function of the amount of Na^+ flow through the cell. Flow rate: 5 ml/min.

exchangers, for example in the cases of tacrine and propranolol [8,9].

4.4. Nadolol

Fig. 5a and b show the experimental and modelled curves for nadolol release with different flow rates and Table 5 shows the corresponding values of *Pe* and *K*. The Peclet numbers decreased with decreasing flow-rate, as the definition of the Peclet number suggests. The release rates of the most hydrophilic

Table 4
Parameters *Pe* and *K* used for the modelling of metoprolol release

	$\dot{V}$ (ml/min)	*Pe*	*K*
Smopex®-102 fiber	5	0.85	250
Smopex®-101 fiber	5	0.70	160
Amberlite IRC-86 gel	5	4.3	17
Diaion WK100 resin	5	4.4	10

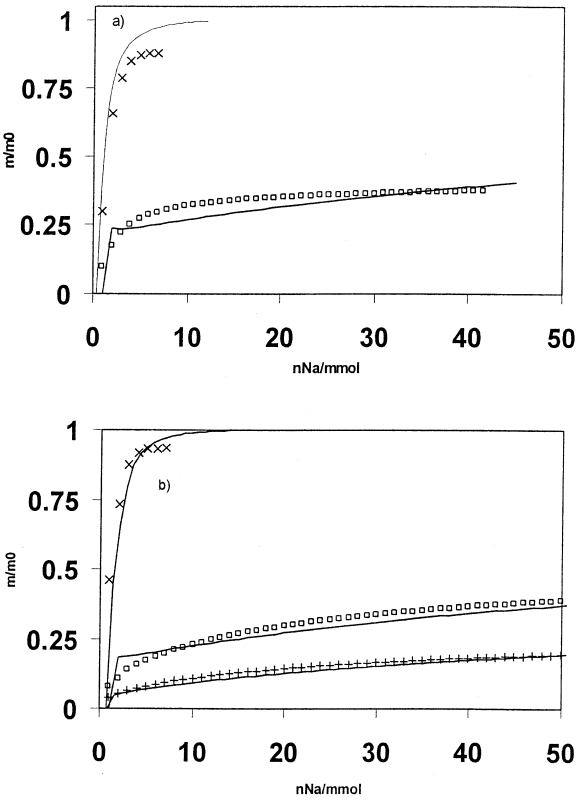

Fig. 5. Experimental [(×) staple 102, (+) gel and (□) resin] and theoretical (———) fractions of nadolol released as a function of the amount of Na^+ flow through the cell. Flow rate: (a) 0.1 ml/min, (b) 5 ml/min.

model drug, nadolol, were clearly higher than for the other model drugs studied. Extremely rapid release of nadolol was evident from the carboxylic acid group-containing staple fiber (Fig. 5a and b). Release of nadolol from the respective gel and resin materials was significantly retarded in comparison to the fiber.

Table 5
Parameters *Pe* and *K* used for the modelling of nadolol release

	$\dot{V}$ (ml/min)	*Pe*	*K*
Smopex®-102 fiber	0.1	0.65	0.70
	5	0.90	0.70
Amberlite IRC-86 gel	5	3.1	110
Diaion WK100 resin	0.1	1.6	106
	1	1.7	106
	5	1.9	106

5. Conclusions

The theoretical model introduced yield values which agree well with the experimental data gathered from the new flow-cell. This indicates that the theory proposed describes the behaviour of these systems adequately. One possible explanation for the small differences between the model and the experimental results is that instead of binding electrostatically to the ion-exchange groups, the drug is adsorbed, e.g. on the surface of the ion-exchange matrix or to the side-chains of other bound drug molecules [31,32]. Also, the assumption that chloride ions are completely excluded from the ion-exchange fiber ignores the influence of the chemical partition coefficient; only the electrostatic interactions are included in the model (see Ref. [9] for details). Thus, nonspecific adsorption of Cl^- ions may contribute, to some extent, to the deviation of the model from the experimental results.

From Figs. 2–5 it can clearly be seen that all the model drugs have much higher release rates from the fiber than from the resin or the gel. The staple form of the fiber gives more rapid release than the cloth form. These differences can be explained by an increase in the surface area (a larger surface area to unit volume ratio) of the ion-exchange matrix and/or a decrease in the diffusion layer thickness, δ, thus allowing the ions rapid access to the ion-exchange groups [2,18]. In general, the *Pe* number was decreased with decreasing flow-rate, as expected from the definition of the Peclet number. These experiments confirm the earlier observation [9] that the release rates from the fiber are higher for the release of hydrophilic drugs (nadolol and metoprolol) and lower for the more lipophilic tacrine and propranolol. The difference in release rates between the fiber or the gel/resin was even greater for more lipophilic drugs.

References

[1] T.S. Stevens, J.C. Davis, Hollow fiber ion-exchange suppressor for ion-chromatography, Anal. Chem. 53 (1981) 1488–1492.

[2] L. Chen, G. Yang, J. Zhang, A study of the exchange kinetics of ion-exchange fiber, React. Funct. Polym. 29 (1996) 139–144.

[3] T. Asami, T. Suehiro, H. Ichijo, A. Yamauchi, S. Ogawa, M. Suzuki, M. Uzumaki, US Patent 4514367, acc. 30.4.1985.

[4] V.S. Soldatov, A.A. Shunkevich, G.I. Sergeev, Synthesis, structure and properties of new fibrous ion exchangers, React. Polym. 7 (1988) 159–172.

[5] D.D. Siemer, Separation of chloride and bromide from complex matrices prior to ion chromatographic determination, Anal. Chem. 52 (1980) 1874–1877.

[6] T.S. Stevens, G.L. Jewett, R.A. Bredeweg, Packed hollow fiber suppressors for ion chromatography, Anal. Chem. 54 (1982) 1206–1208.

[7] P.K. Dasgupta, Annular helical suppressor for ion chromatography, Anal. Chem. 56 (1984) 103–105.

[8] T. Jaskari, M. Vuorio, K. Kontturi, A. Urtti, J.A. Manzanares, J. Hirvonen, Controlled transdermal iontophoresis by ion-exchange fiber, J. Controlled Release 67 (2000) 179–190.

[9] T. Jaskari, M. Vuorio, K. Kontturi, J.A. Manzanares, J. Hirvonen, Ion-exchange fibers and drugs: an equilibrium study, J. Controlled Release 70 (2001) 219–229.

[10] T. Kankkunen, R. Sulkava, M. Vuorio, K. Kontturi, J. Hirvonen, Transdermal iontophoresis of tacrine in vivo, Pharm. Res. 19 (2002) 705–708.

[11] T. Tomida, T. Inoue, K. Tsuchiya, S. Masuda, Concentration and/or removal of metal ions using a water-soluble chelating polymer and a microporous hollow fiber membrane, Ind. Eng. Chem. Res. 33 (1994) 904–906.

[12] E. Kucera, Contribution to the theory of chromatography linear non-equilibrium elution chromatography, J. Chromatogr. 9 (1965) 237–248.

[13] M. Suzuki, J.M. Smith, Kinetic studies by chromatography, Chem. Eng. Sci. 26 (1971) 221–235.

[14] V.V. Krongautz, C.W. Kocher, Kinetics of ion exchange in monodisperse resin, J. Appl. Polym. Sci. 67 (1997) 1271–1283.

[15] M. Chanda, G.L. Rempel, Gel-coated ion-exchange resin: a new kinetic model, Chem. Eng. Sci. 54 (1999) 3723–3733.

[16] G. Schmuckler, Kinetics of moving boundary ion-exchange processes, React. Polym. 2 (1984) 103–110.

[17] M. Streat, Kinetics of slow diffusing species in ion exchangers, React. Polym. 2 (1984) 79–91.

[18] W. Lin, Y.L. Hsieh, Kinetics of metal ion absorption on ion-exchange resins and chelating fibers, Ind. Eng. Chem. Res. 35 (1996) 3817–3821.

[19] S.J. Zhou, Ion Exch. Absorpt. 5 (1987) 51, in Chinese; cited in Ref. [2].

[20] T. Miyamatsu, Fibrous ion exchanger and its application, Sen'I Gakkaishi 39 (1983) 53, cited in Ref. [4].

[21] M. Takashio, Characteristics and use of ion exchange fibres, Kogyo Zairyo 31 (1983) 102, cited in Ref. [4].

[22] L.A. Wolf, Modified fibres of specific properties, Chem. Ind. 3 (1983) 134, in Bulgarian; cited in Ref. [4].

[23] L.A. Wolf, Fibres of Specific Properties, Khimiya, Moscow, 1980, in Russian; pp. 240; cited in Ref. [4].

[24] F.G. Helfferich, Ion exchange kinetics. V. Ion exchange accompanied by reactions, J. Phys. Chem. 69 (1965) 1178–1187.

[25] P.B. Weisz, R.D. Goodwin, Combustion of carbonaceous

deposits within porous catalyst particles. I. Diffusion controlled kinetics, J. Catal. 2 (1963) 397–404.
[26] M. Chanda, G.L. O'Driscoll, K.F. Rempell, Removal of copper and silver from dilute aqueous solutions using mercaptoacetimide of poly(ethyleneimine) and poly-(propyleneimine), React. Polym. 4 (1986) 213–223.
[27] A. Fernández, C. Suárez, M. Díaz, Kinetics of metal ion exchange in iminodiacetic resins at low concentrations, J. Chem. Technol. Biotechnol. 58 (1993) 255–260.
[28] F.G. Helfferich, Models and physical reality in ion-exchange kinetics, React. Polym. 13 (1990) 191–194.
[29] F.G. Helfferich (Ed.), Ion Exchange, Dover Publications, New York, 1995, pp. 252–257.
[30] H. Vihola, A. Laukkanen, J. Hirvonen, H. Tenhu, Binding and release of drugs into and from thermosensitive poly(*N*-vinylcaprolactam) nanoparticles, Eur. J. Pharm. Sci. 16 (2002) 69–74.
[31] O.M. Conaghey, J. Corish, O.I. Corrigan, Iontophoretically assisted in vitro membrane transport of nicotine from a hydrogel containing ion-exchange resins, Int. J. Pharm. 170 (1998) 225–237.
[32] L. Marchal-Heusser, N. Colling, E. Benoit, P. Maincent, J. Bessierre, Applicability of dielectric measurements to the adsorption of beta blockers onto a pharmaceutical grade ion-exchange resin, Pharm. Res. 17 (2000) 1144–1147.
[33] C.J. Crayton, Cumulative subject index and drug compendium, in: C. Hansch, P.G. Sammes, J.B. Taylor (Eds.), Comprehensive Medicinal Chemistry, Vol. 6, Pergamon Press, Oxford, 1990.